35th Annual International Conference of the IEEE EMBS
Osaka, Japan, 3 - 7 July, 2013

Ultrasound Lesion Segmentation Using Clinical Knowledge-Driven Constrained Level Set

QiZhong Lin, Sheena Liu, Shyam Sundar Parajuly, Yinhui Deng,
Lilla Boroczky, Sainan Fu, Ying Wu, Yulan Pen

Abstract— **Ultrasound lesion segmentation is an important and challenging task. Comparing with other methods, region-based level set has many advantages, but still requires considerable improvement to deal with the characteristic of lesions in the ultrasound modality such as shadowing, speckle and heterogeneity. In the clinical workflow, the physician would usually denote long and short axes of a lesion for measurement purpose yielding four markers in an image. Inspired by this workflow, a constrained level set method is proposed to fully utilize these four markers as prior knowledge and global constraint for the segmentation. First, the markers are detected using template-matching algorithm and B-Spline is applied to fit four markers as the initial contour. Then four-marker constrained energy is added to the region-based local level set to make sure that the contour evolves without deviation from the four markers. Finally the algorithm is implemented in a multi-resolution scheme to achieve sufficient computational efficiency. The performance of the proposed segmentation algorithm was evaluated by comparing our results with manually segmented boundaries on 308 ultrasound images with breast lesions. The proposed method achieves Dice similarity coefficient 89.49±4.76% and could be run in real-time.**

I. Introduction

Breast cancer is the second leading cause of death of women worldwide [1]. To reduce mortality rate early detection followed by effective treatment is crucial. Ultrasound is often the first-line screening and diagnosis modality in low-resource countries as it is more sensitive to dense breasts and more accessible. Since ultrasound imaging is much more operator-dependent than mammography, interpreting ultrasound images requires high-level of experience. Therefore, clinical decision support (CDS) tools, such as computer-aided diagnosis (CADx) [2] and similar case retrieval from a database [3] have been developed to assist less-experienced radiologists in making accurate diagnosis.

Lesion segmentation is an important step in CADx/CDS systems because many crucial features for discriminating benign and malignant lesions are related to lesion shape and margin. However, the artifacts, such as attenuation, speckle, shadowing, non-uniform contrast of certain structures and high variability of the echogenicity of the lesion, make lesion segmentation a challenging task. Many approaches for ultrasound image segmentation [4-9] have been proposed in the past with various levels of success. One common issue is that without sufficient prior knowledge, the iterative energy propagation would be trapped into local minimum and would fail to delineate the true boundary of lesions when the artifacts are present. In the present work, inspired by the clinical workflow where physicians often identify lesions with four markers, we derived a knowledge-enriched segmentation framework. The four markers associated with long and short axes of a lesion, are used as prior knowledge and global constraint to facilitate the lesion segmentation. First, the four markers are detected automatically. Next, B-Spline is applied to fit the four markers as the initial contour. Then, four-marker constrained energy is added to the region-based local level set [8-9] to make sure that the contour evolves without deviation from the four markers. Finally, the algorithm is implemented in a multi-resolution scheme to achieve acceptable processing time. We demonstrated the improved performance of our algorithm by comparing the segmentation results with manually segmented boundaries and other segmentation methods [6-7].

Qizhong Lin is with Philips Research Asia Shanghai, Shanghai, China (corresponding author, phone: 86-21-24115296; fax: 86-21-54452890; e-mail: QiZhong.Lin@ Philips.com).

Sheena Liu and Lilla Boroczky are with Philips Research North America, Briarcliff Manor, NY, USA.

Shyam Sundar Parajuly and Yulan Pen are with Department of Ultrasound, Western China Hospital, Chengdu, China.

Yinhui Deng, Sainan Fu and Ying Wu are with Philips Research Asia Shanghai, Shanghai, China.

II. Database

The breast ultrasound database was constructed from 2011 to 2012 from the Ultrasound Department of the Western China Hospital (Chengdu, China) with the consent of all patients. All data were de-identified. The database consists of 308 pathology-proven ultrasound cases including 194 benign and 114 malignant breast lesions. In each case there are multiple images scanned from different angles and positions among which there is one image with four markers to denote long and short axes of a lesion. All digital ultrasound images were obtained using Philips iU22 ultrasound system and stored in DICOM format. The capturing resolution of the ultrasound images was 1024×728 pixels. Each monochrome ultrasound image was quantized into 8 bits with 256 gray levels. Ground truth segmentation was provided by delineating each lesion manually by one physician (a co-author (S.S.P.)), with 10-year of experience in interpreting ultrasound breast images. For the difficult cases, in order to study variability between different human observers, 30 cases were segmented manually by two other physicians: one expert and one junior physician with more than 25-year of experience, and less than 5-year of experience in interpreting ultrasound breast images, respectively. In these 30 cases, the manual contour of the most senior physician is considered as ground truth.

978-1-4577-0216-7/13/$26.00 ©2013 IEEE

III. METHOD

In the clinical workflow, physicians have to first identify a lesion, then input two markers (e.g. cross) to measure the long axis of a lesion and two other markers (e.g. star) to measure the short axis of the lesion. Based on this workflow, we first detect the four markers from the images, then, utilize these four markers to generate an initial curve via B-Spline fitting. Next, four-marker constrained level-set is used to segment the lesion boundary. If the markers are absent or could not be detected, the users are prompted to first draw the short/long axis of the tumor, and then the proposed segmentation method is triggered. The flow-chart of the proposed lesion segmentation is shown in Figure 1.

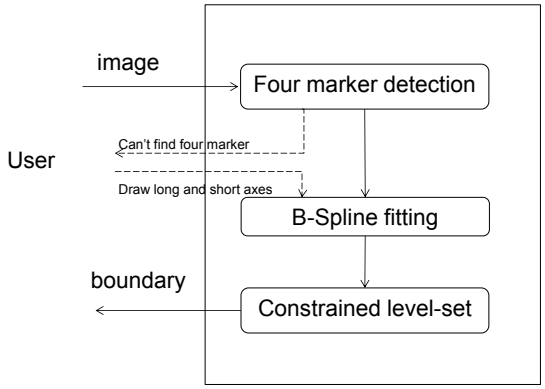

Figure 1. The flow-chart of the proposed lesion segmentation

A. Detection of four markers

To automatically detect the four markers, the following algorithm was applied:

a) Detect the ultrasound echo data region (the region with image content) from the original DICOM image

b) Create a binary image of the ultrasound echo data region

c) Detect markers based on rotational symmetry with respect to the centroid

d) Detect two types of high-quality (not noisy) markers

e) Test whether long and short axes intersect with each other to remove false markers

Most markers present rotational symmetry. In order to detect markers fast and robustly, the 2-dimensional markers are projected into 1-dimension via radon transformation. Based on the projection angle and the number of modes exist in different projection space, we are able to differentiate different types of makers In case when markers are noisy (in our dataset about 5% of the cases) and are outside of the echo data, template matching algorithm is applied. The formula of normalized cross-correlation between the template and the image is given as below:

$$\gamma(\Delta m,\Delta n)=\frac{\sum_{x,y}\left[I(x,y)-\bar{I}_{u,v}\right]\left[t(x-\Delta m,y-\Delta n)-\bar{t}\right]}{\left\{\sum_{x,y}\left[I(x,y)-\bar{I}_{u,v}\right]^2\sum_{x,y}\left[t(x+\Delta m,y+\Delta n)-\bar{t}\right]^2\right\}^{0.5}}$$

where I is the image, t is the template, $\bar{t}$ is the mean of the template, $\bar{I}$ is the mean of $I(x,y)$ in the region under the template. The similarity measure between the template and the image is computed and has a value between -1 and +1.

B. Four-marker constrained level set method

As Chan and Vese mentioned in [10], global region-based active contour method models the foreground and background regions statistically and find an energy optimum where the model best fits the image. Assuming that the image $I(x,y)$ is formed by the foreground and background, the energy function $F(u,v,C)$ is defined as

$$F(u,v,C)$$
$$=\mu\cdot L(C)+k\cdot A\big(inside(C)\big)+r_1\int_{inside(C)}|I(x,y)-u|^2dxdy$$
$$+r_2\int_{outside(C)}|I(x,y)-v|^2dxdy$$

where C is the evolving contour, u and v are the mean values of image intensities inside and outside C, respectively, μ, k, r_1 and r_2 are fixed parameters which should be larger than zero, $L(C)$ is the length of the curve C, $A\big(inside(C)\big)$ is the area of the inside region. The first two terms are regularizing and the last two terms are internal energy terms.

However, global region-based active contour that models the object using global statistics cannot segment heterogeneous objects correctly which frequently occur in ultrasound breast images. Using only global statistics would lead to boundary leak.

Lankton and Tannenbaum [8] proposed a local region-based active contour method which allows the foreground and background to be described in local areas instead of in one global area, which leads to the construction of a family of local energies at each point along the curve. Each local area is split into local interior and exterior areas by the evolving curve computing the local energy. The total internal energy is the sum of local energy for every local area along the evolving curve. Assuming that the image $I(x,y)$ is defined on the domain Ω, and C be a closed contour represented as the zero level set of a signed distance function $\emptyset$, $i.e.$, $C=\{(x,y)|\emptyset(x,y)=0\}$, the interior of C is specified by the following approximation:

$$H\big(\emptyset(x,y)\big)=\begin{cases}1, & \emptyset(x,y)<-\epsilon\\ 0, & \emptyset(x,y)>\epsilon\\ \frac{1}{2}\left\{1+\frac{\emptyset}{\varepsilon}+\frac{1}{\pi}sin\left(\frac{\pi\emptyset(x,y)}{\epsilon}\right)\right\}, & otherwise\end{cases}$$

The exterior of C is defined as (1- $H\big(\emptyset(x,y)\big)$). The area just around the curve could be denoted by the following function:

$$\delta\left(\emptyset(x,y)\right)=\begin{cases}1, & \emptyset(x,y)=0\\ 0, & |\emptyset(x,y)|<\epsilon\\ \frac{1}{2\epsilon}\left\{1+\cos\left(\frac{\pi\emptyset(x,y)}{\epsilon}\right)\right\}, & otherwise\end{cases}$$

The energy function is defined as

$$E(\emptyset) = \int_{\Omega_m} \delta(\emptyset) \int_{\Omega_n} B(m,n) F\big(I(m), \emptyset(m)\big) dn dm + \gamma \int_{\Omega_m} \delta(\emptyset) \|\nabla \emptyset(m)\| dm$$

where $B(m,n) = \begin{cases} 1, & \|m-n\| < r \\ 0, & \|m-n\| \geq r \end{cases}$ is the mask of local regions, m is the first spatial variable to replace (x, y) and n is the second spatial variable. $B(m,n)$ will be 1 when the point n is within a ball of radius r centered at m. $F\big(I(m), \emptyset(m)\big)$ is the internal energy like Chan and Vese's internal energy. The second term is a regularization term.

Local region-based active contour that models the object using local statistics can segment heterogeneous objects correctly, but is sensitive to the initial curve and overlapping intensity between foreground and background. In addition, the accuracy is dependent on the size of the predefined local region. Furthermore, the computation can be time-consuming.

Thus, in our approach, first, we use B-spline fitting on the four markers to create an initial contour, which could be much closer to the true lesion boundary.

Then, to improve the local region-based active contour, four constrained energies centered at four markers are added to the total active contour energy to ensure contour evolving without deviation from the four corners. These constrained terms are defined as Gaussian functions:

$$G(x,y) = \sum_{i=1}^{4} -\emptyset(x,y) \cdot \lambda \cdot e^{\frac{(x-x_i)^2+(y-y_i)^2}{2\sigma}}$$

where (x_i, y_i) is the position of marker, λ is the height of the Gaussian, σ is the standard deviation which is set as half of short axes of the lesion.

Finally, the proposed segmentation algorithm was implemented in a multi-resolution scheme, where the segmented lesion boundary in the coarse level is used as the initial contour for the subsequent finer level applying linear interpolation. The final segmentation result for the lesion is obtained in the finest level. The number of the decomposition level is automatically adjusted according to the size of the lesion, the maximum number of the decomposition level is 3.

IV. Results

The performance of the segmentation algorithm is assessed by comparing the computer-segmented contour with the manual-segmented boundary. Four similarity measures, i.e., Dice similarity coefficient (DSCE), miss fraction (MF), extra fraction (EF) [8] and Hausdorff distance (HD) [12], were calculated for quantitative analysis of the segmentation result. These measures are defined as the following:

$$DSCE = 2 * (REF \cap SEG)/(REF + SEG)$$
$$MF = 2 * (REF \cap \overline{SEG})/(REF + SEG)$$
$$EF = 2 * (\overline{REF} \cap SEG)/(REF + SEG),$$

where SEG and REF denote the area enclosed by the computer- segmented region and by the manual-segmented region, respectively. The larger DSCE the result has, the more overlapping the two regions have. With the smaller MF, the less lesion part is missing; and with the less EF, the less normal tissue part is falsely segmented as lesion. The Hausdorff distance is to determine the degree to which two shapes differ from one another. Assuming two point sets $A = \{a1, \cdots, ap\}, B = \{b1, \cdots, bq\}$ defining two contours of segmentations, the Hausdorff distance $HD(A, B)$ is defined as $\max(h(A, B), h(B, A))$ while

$$h(A, B) = \max_{a \in A} \min_{b \in B} \|b - a\|_2$$

To test the proposed marker detection algorithm, we have used 308 images with four markers and 1501 images without four markers. To test the proposed constrained level set algorithm, 308 images were used to compare computer-segmented contours with manual-segmented boundaries.

The sensitivity and specificity of the marker detection was 100% and 100%, respectively.

Figure 2 shows an example lesion segmented by the proposed and other methods [6-7]. Table I summarizes the quantitative segmentation results for the proposed and other approaches. It can be seen that better results were achieved by our proposed method. In the 30 difficult cases, our algorithm delivers comparable segmentation accuracy with respect to contours created by the expert physician (see Table II).

The test platform was CPU Intel® Xeon® X5672 @3.20GHz with 4 cores, RAM of 8 GB and 64-bit operating system. With multi-resolution and C++ multi-threading configuration, the proposed method takes about 0.5~1.5 second to segment a breast lesion in one image depending on the size of the lesion.

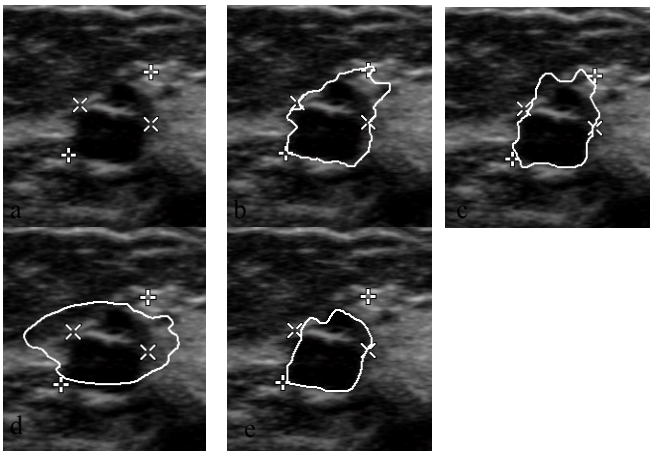

Figure 2. Results of lesion segmentation: (a) is the original image with four markers which were used to denote long and short axes of the lesion, (b) manual-segmented lesion, (c) segmentation by the proposed method (d) Giger2001's result [6]. (e) GVF-Snake's result [7].

TABLE I. QUANTITATIVE RESULT OF LESION SEGMENTATION BASED ON 308 CLINICAL IMAGES WITH GROUND TRUTH (MANUAL) SEGMENTATION

	DSCE (%)	MF (%)	EF(%)	HD
Our method	89.49±4.76	13.12±7.36	6.04±6.79	36.14±25.97
GVF-Snake	79.94±8.81	13.99±9.95	29.86±17.9	60.09±28.71
Giger2001	78.87±11.61	10.80±12.87	35.86±49.36	56.08±31.51

Note: the result is denoted as mean±std * 100%.

TABLE II. COMPARISON OF THE PROPOSED SEGMENTATION WITH MANUAL SEGMENTATION OF EXPERTS FOR THE 30 DIFFICULT CASES

	DSCE (%)	MF (%)	EF(%)	HD
a)	85.89±7.14	9.05±9.15	22.05±22.66	70.31±43.68
b)	87.16±7.19	9.15±9.26	18.5±20.54	63.97±47.40
c)	85.00±7.42	15.65±12.12	13.92±15.61	82.25±57.22

Note: manual contour of the most senior physician (25-year experience) is considered as ground truth; a) results from the junior physician (5-year experience); b) results from the expert physician (10-year experience); c) results from the proposed method.

V. DISCUSSION

In this paper, we use ultrasound breast lesion segmentation as an example to demonstrate a clinical workflow-driven segmentation scheme. This automatic lesion segmentation method incorporates the essential elements that are indispensable part of the clinical workflow, and thus improve the segmentation accuracy considerably. The proposed approach achieves segmentation performance with DSCE 89.49% for the 308 cases. For the difficult 30 cases (out of the total database), the proposed method achieves comparable performance as that of a junior physician at least based on DSCE. After a discussion with a senior physician, the intrinsic reasons that would contribute to the challenges in segmentation of these difficult cases are: 1. some malignant lesions do not have capsule, thus there is no clear boundary between the lesion and surrounding tissue. 2. there might exist inflammation area between lesion and normal tissue. One major limitation of our algorithm is the assumption that the four markers are placed approximately in the lesion boundary by a physician.

The above preliminary results have shown promise in segmenting breast lesions exhibiting variety of appearance. Future work would be to extend this framework to 3D and to ultrasonic images of other organs. For 3D lesion segmentation, a physician most likely will be asked to place more markers then four on the image volume.

REFERENCES

[1] P. Parkin, D.M. Parkin, F.I. Bray et al. "Estimates of the worldwide mortality from 25 major cancers in 1990. Implications for prevention, and projections of future burden." *Int J Cancer*, vol. 83, pp. 18-29, Sep. 1999.

[2] K. Drukker, N.P. Gruszauskas, C.A. Sennectt, and M.L. Giger. "Breast US computer-aided diagnosis workstation: performance with a large clinical diagnostic population". *Radiology*, vol. 248, pp. 392-397, Aug. 2008.

[3] H.C. Cho, L. Hadjiiski, S. Berkman, H.P. Chan, H. Mark, P. Chintana and A.V. Nees. "Similarity evaluation in a content-based image retrieval (CBIR) CADx system for characterization of breast masses on ultrasound images". *Med. Phys.,* vol. 38, pp. 1820-1831, April 2011.

[4] H.D. Cheng, J. Shan, W. Ju, Y.H. Guo and L. Zhang. "Automated breast cancer detection and classification using ultrasound images: A survey". *Pattern Recognition*, vol. 43, pp. 299-317, Jan. 2010.

[5] J.A. Nobel, B. Djamal. "Ultrasound image segmentation: A survey". *IEEE Transactions on Medical Imaging*, vol. 25, pp. 987-1010, Aug. 2006.

[6] K. Horsch, M.L. Giger, L.A. Venta and C.J. Vyborny. "Automatic segmentation of breast lesions on ultrasound". *Med. Phys.,* vol. 28, pp. 1652-1659, Aug. 2001

[7] C.Y. Xu and L.P. Jerry. "Gradient vector flow: a new external force for snakes". *In Proceedings, 1997 IEEE Computer Society Conference on Computer Vision and Pattern Recognition,* 1997. pp. 66-71.

[8] S. Lankton and A. Tannenbaun. "Localizing region-based active contours". *IEEE Transactions on Image Processing ,* vol. 17, pp. 2029-2039, Nov. 2008

[9] Y.L. Huang, Y.R. Jiang, D.R. Chen and W.K. Moon. "Level set contouring for breast tumor in sonography". *Digital Imaging,* vol. 20, pp. 238-247, Sep. 2007

[10] T.F. Chan, L.A. Vese. "Active contour without edges". *IEEE transactions on image processing,* vol. 10, pp. 266-277, Feb. 2001

[11] J.Shan, H.D.Cheng and Y.X.Wang. "A novel automatic seed points selection algorithm for breast ultrasound images". *In Proceedings of International Conference on Pattern Recognition,* Tampa, Finland, 2008, pp. 1-4.

[12] P.H. Daniel, A.K. Gregory and J.R. William. "Comparing images using the hausdorff distance". *IEEE transactions on pattern analysis and machine intelligence,* Vol. pp.850-863, Sep. 1993